Focusing a shock wave;
microscopic structure of the phenomenon

Z. A. WALENTA and J. ORZEŃSKI (WARSZAWA)

THE PROBLEM OF FOCUSING a shock wave after its reflection from a concave wall is considered experimentally (in a shock tube) and numerically (employing the Direct Simulation Monte–Carlo technique). Rarefied flow conditions make it possible to clarify both the size of the focus and the structure of its neighbourhood.

1. Introduction

THE PROCESS OF FOCUSING of a shock wave was investigated by a number of researchers for many years (see e.g. [1, 2, 4] and the papers cited there). The interest was related mainly to its possible applications (military, medical, industrial etc.), however the phenomenon itself can offer some advantages of a more fundamental nature (possibility of producing the medium in the state very far from thermodynamic equilibrium).

There are several methods of focusing the shock wave. The one used in the first (to our knowledge) experiment on this subject, was proposed by PERRY and KANTROWITZ [1]. A plane shock wave, generated in a shock tube of circular cross-section, is transformed into a ring-shaped one by an axisymmetric inner body, placed at the axis of the tube. Having reached the gap between the inner body and the end plate of the tube, the shock turns towards the axis, becomes cylindrical and eventually, focuses.

This method allows in principle to produce a nearly perfect focus, where the parameters of the gas (pressure, temperature) are very high. Unfortunately it is plagued by the inherent instabilities of the converging shock. Moreover, because of the geometrical complexity, this method cannot be applied to many problems of practical interest.

The method most frequently used, is based on reflection of a plane, or spherical, divergent shock wave from a suitably shaped concave reflector (paraboloidal or ellipsoidal, respectively) [2, 3, 4]. This method is simpler in realization, but produces "foci" of larger size.

The present study is concerned with investigation of the mechanism of focusing of the plane shock after reflection from a concave wall. Such configuration was extensively studied in the past, however the experiments were always performed at relatively high densities and the description was based on the model of continuous medium, in which the shock was assumed to be infinitely thin.

Therefore the problem of the structure of the focusing shock and the focus itself – the main aim of the present paper – was never considered.

In their fundamental paper "The focusing of weak shock waves" STURTEVANT and KULKARNY [2] distinguish between the case of very weak shocks, for which "the wavefronts emerge from focus crossed and folded, in accordance with the predictions of geometrical acoustics theory" and the strong–shock case, for which "the fronts beyond focus are uncrossed, as predicted by the theory of shock dynamics". In the present study we shall concentrate only on the strong shock case because detection of weak shock waves at low gas densities faces great experimental difficulties.

2. Experiment

2.1. Apparatus and procedure

The problem formulated above required the apparatus suitable for low-density experiments. The shock tube of the Institute of Fundamental Technological Research, Polish Academy of Sciences, Warsaw, was selected for this purpose. This tube, [5], especially designed for work in the rarefied gas regime, is of 250 mm internal diameter and about 17 meters length. Such dimensions are needed to work at densities, corresponding to mean free paths of the gas particles of the order of 1 mm, without too strong, disturbing influence of the boundary layer, generated at the shock tube walls.

Inside the test section of the tube a plane, parabolic reflector was placed (Fig. 1). The reflector was made of aluminum. Its span was equal to 210 mm, its depth – 45 mm, which produced the "geometrical focal length" 61.25 mm. The width of the reflector (in the direction perpendicular to the picture) was equal to 136 mm. To maintain the planarity of the flow, the reflector was placed between two aluminum plates, extending 75 centimeters upstream of the test section.

After interaction with reflector of such a shape, the shock wave converged and produced a "linear focus" at the plane of symmetry of the reflector.

The measurements were performed with the standard, electron beam attenuation technique [6]. The beam (of about 0.5 mm thickness) was perpendicular to the tube axis and parallel to the reflecting surface. Position of the beam with respect to the reflector could be varied. The maximum distance of the beam from the reflector in the direction of the tube axis was equal to about 60 mm; the minimum distance was about 2.4 mm (as the distance of the electron beam from the solid wall must be large enough to avoid the disturbing influence of the wall on the measurement). The maximum distance of the beam from the plane of symmetry was 10 mm. The field of observation defined in this way was large enough to investigate the structure of the shock focus.

For one experiment, a number of runs at the same flow conditions and different locations of the beam relative to the wedge was done. In a single run
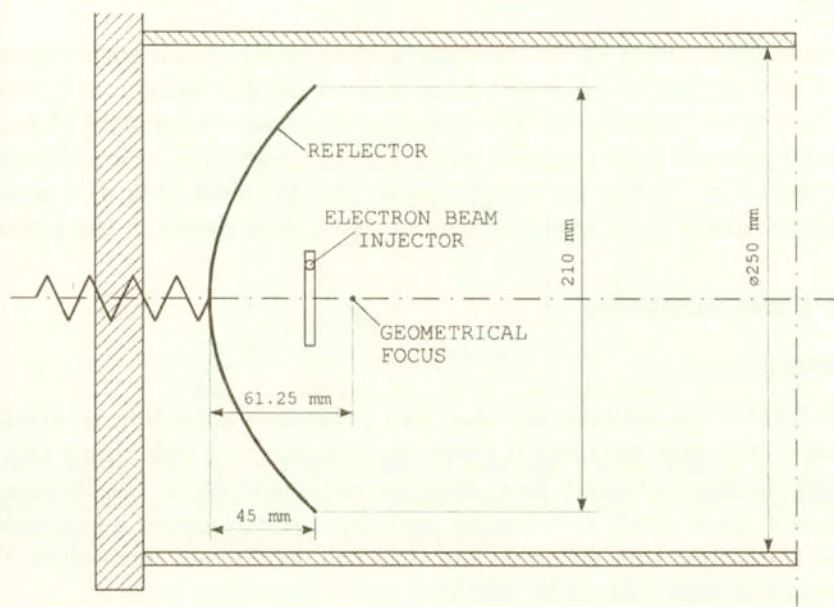
FIG. 1. Shock tube with a parabolic reflector mounted inside.

the density history at one point in the flow was recorded (compare Fig. 3). To obtain the momentary picture of the density field, the results were then recalculated with suitable numerical procedure. The reference time instant, necessary for superposition of the results, was provided in each run by a laser differential interferometer, placed at a fixed point in front of the reflector.

Meaningful results were obtained when the neighbouring locations of the beam were, at the most, one shock wave thickness apart. A special care was needed to maintain good repeatability of the flow conditions. The obtained scatter of shock speeds, ± 2.5 per cent of the mean value, was sufficiently small from this point of view.

2.2. Conditions of the experiment

The conditions of experiment were selected as follows:
- argon (spectrally pure) was used as the test gas;
- the shock Mach number (Ms) was 1.60 ± 0.03;
- the initial pressure – 7.33 Pa;
- the initial temperature (equal to room temperature) – 298 ± 1 K.

For such conditions the mean free path of the gas atoms was about 0.95 mm, which enabled us to investigate the shock structure with the electron beam of 0.5 mm diameter (the maximum slope thickness of the incident shock was equal to about 7 mm [7]).

2.3. Accuracy

The possible inaccuracy of the position of the electron beam with respect to the wedge was estimated to be about 0.1 mm in the axial direction, as vell as in the direction perpendicular to it. The inaccuracy of the measurement of density was about ± 5 per cent of the current value. The resulting inaccuracy of position of any constant density line in the picture of the flow field (Fig. 4) was lower than half of the distance between the neighbouring lines shown in the picture.

3. Monte–Carlo simulation

3.1. The method

For the DSMC calculations the standard procedure according to BIRD [8] was employed. The flow field was divided into a number of cells. Each cell was chosen small enough to neglect flow nonuniformities inside it. The flowing gas was represented by a number of "model particles", which moved along straight lines during prescribed time intervals and then collided among themselves. Only particles from the same cell could collide.

To simulate the particles the Hard Sphere (HS) model was used. Selection of particles for collision was performed with the ballot-box scheme, proposed by YANITSKIY [9]. Interactions of the particles with physical boundaries were simulated, following MAXWELL [10], with the concept of accommodation coefficient:

$$\alpha = \frac{n_d}{n_d + n_s},$$

where n_d – number of molecules reflected diffusely at the surface, n_s – number of molecules reflected specularly, $n_d + n_s$ – total number of reflected molecules.

If the particle hit the boundary on its way, a random number of molecules was generated. In case when its value was smaller than α, the particle was allowed to reflect specularly, otherwise – diffusely. Total number of cells in the calculations never exceeded 32400; total number of the model particles could not be larger than 160000. The results were averaged over 100 to 500 calculation runs and then smoothed, following the procedure suggested by HONMA et al. [11].

3.2. Details of calculation

The matrix of cells employed in the calculations was rectangular. All cells, except those neighbouring the reflector, had the same dimensions: 0.5λ in the direction of wave propagation and 0.8λ in the direction perpendicular to it (λ is the mean free path in the undisturbed gas). The cells neighbouring the reflector were smaller than that; their shapes and sizes resulted from cutting off a part of the original rectangle by the curved reflecting surface (Fig. 2).

The accommodation coefficient at the reflecting surface was assumed to be equal to $\alpha = 0.3$. Such a value was selected on the basis of the previously
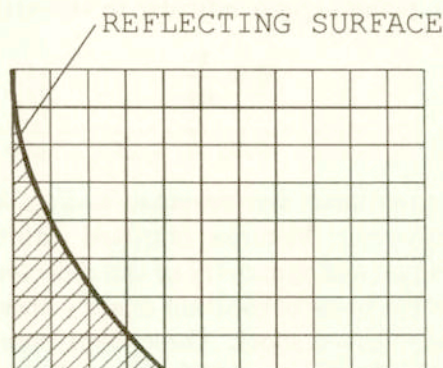
REFLECTING SURFACE

FIG. 2. Cell pattern for DSMC calculations.

obtained results for regular reflection of the shock from the wedge [12]. At the sidewalls, specular reflection of the molecules (accommodation coefficient $\alpha = 0$) was assumed for the majority of calculations.

4. Results

4.1. Form of presentation

The results are presented in the form of isolines of density, temperature, pressure and velocity at the front side of the reflector, for several subsequent time instants. The diagrams of the shock wave structure, showing the distributions of gas density inside the shock, are also shown.

The gas parameters are expressed in non-dimensional form:
Density

$$\overline{\varrho} = \frac{\varrho - \varrho_1}{\varrho_2 - \varrho_1},$$

where ϱ is the current density value, subscripts 1 and 2 correspond to the values in front and behind the incident shock, respectively.

Temperature

$$\overline{T} = \frac{T - T_1}{T_2 - T_1}.$$

Pressure

$$\overline{p} = \frac{p - p_1}{p_2 - p_1}.$$

Horizontal velocity component (parallel to the axis of symmetry)

$$\overline{u} = \frac{u}{u_2}$$

(the velocity in front of the incident shock equals zero).

Vertical velocity component (perpendicular to the axis)

$$\overline{v} = \frac{v}{u_2}.$$

4.2. Experiment

The results of the experiment are presented in Figs. 3–6. Figure 3 presents five examples of the raw density histories, obtained with the electron beam densitometer, placed in the plane of symmetry of the reflector at five distances from its apex. Figure 4 shows the maps of constant density lines for five (evenly spaced in time) positions of the reflected shock. These maps were obtained from density traces, like those shown in Fig. 3, recorded for about 100 positions of the densitometer with respect to the reflector. Figure 5 (solid line) presents the diagram of the reflected shock trajectory and, finally, Figure 6 shows the density diagrams inside the shock (shock wave structures) for the same positions as Fig. 4.
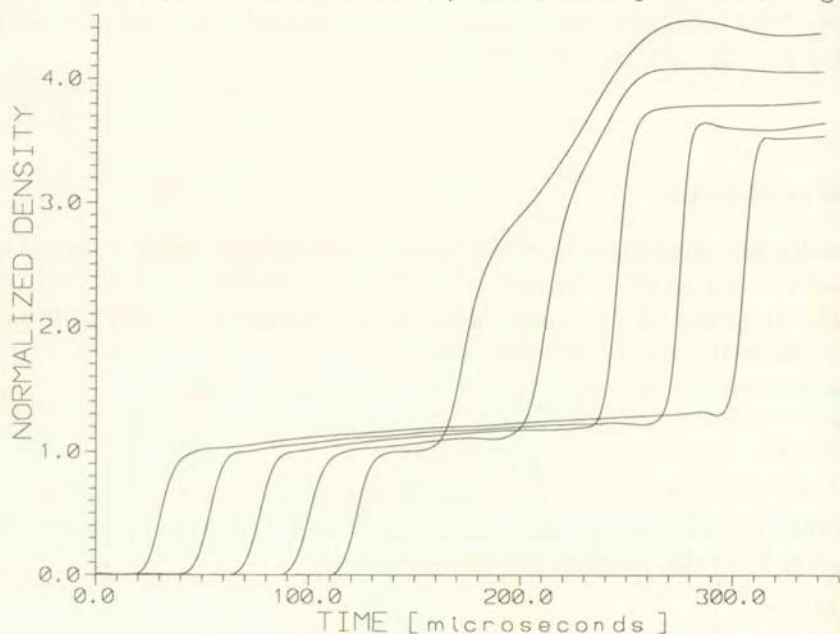

FIG. 3. Density histories at five points on the axis of the reflector (from experiment).

The constant density lines (Fig. 4) do not exhibit strong curvature. The reflected shock wave velocity varies only slightly, as one can infer from the fact, that the shock wave trajectory (Fig. 5, solid line) is close to a straight line. Similarly, the variation of the density increase across the reflected shock (Fig. 6) is not strong.

These findings could not be understood without the information on the whole flow field, not only the area close to the plane of symmetry of the reflector. To gain this information we used the Monte–Carlo numerical calculations.
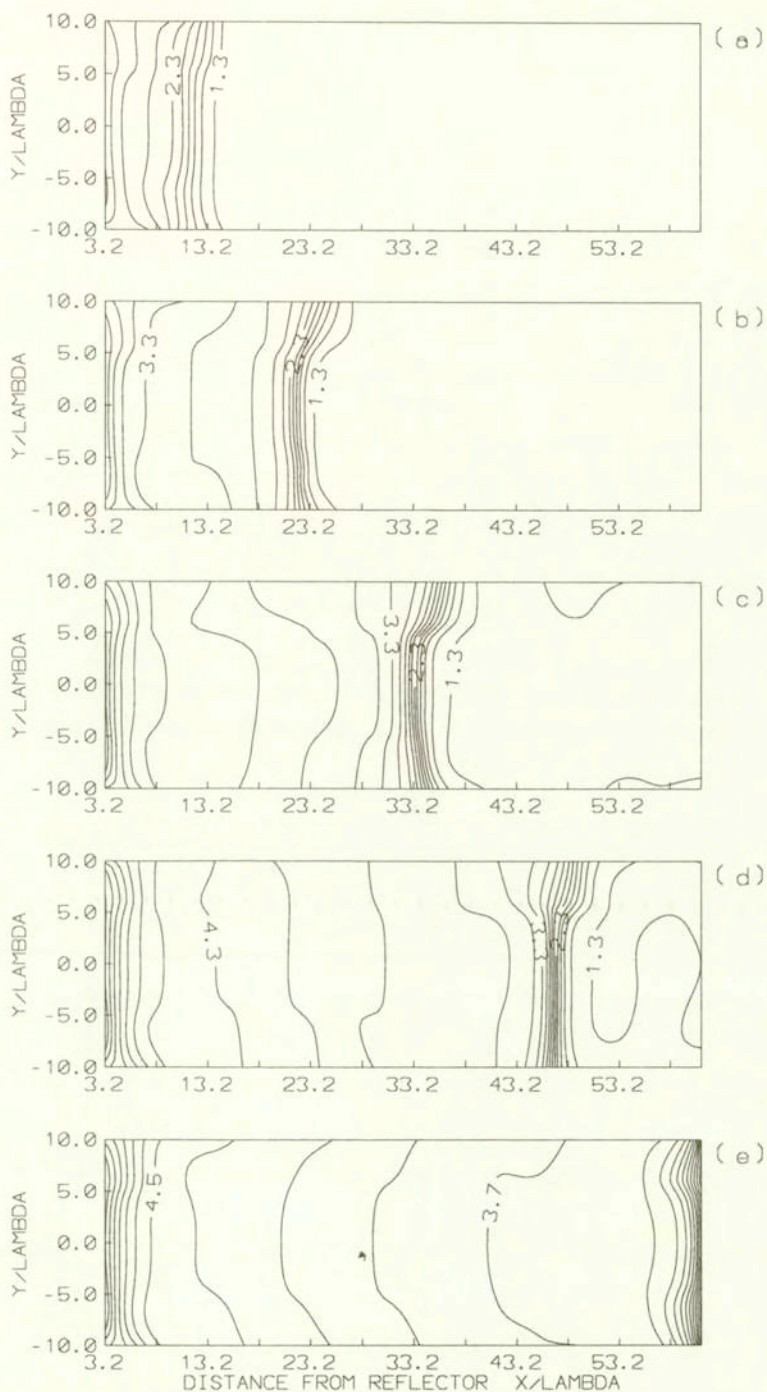
FIG. 4. Constant normalized density contours ($\bar{\varrho}$) for five positions of the reflected shock (from experiment). Distances from the apex of the reflector to the centre of the reflected shock equal to: a) 11.8λ, b) 21.8λ, c) 33.2λ, d) 46.9λ, e) 60.8λ (λ – mean free path of the particles in the undisturbed gas).
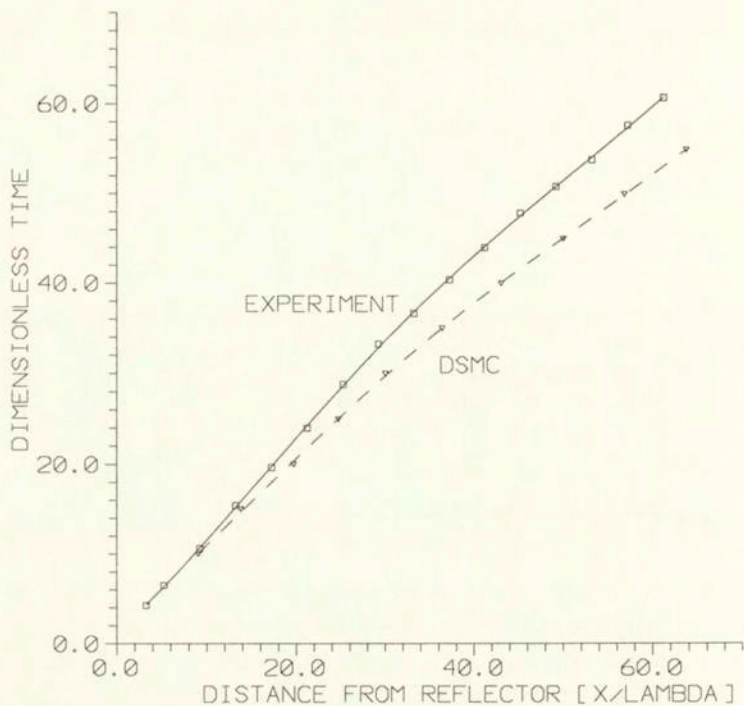
[271]

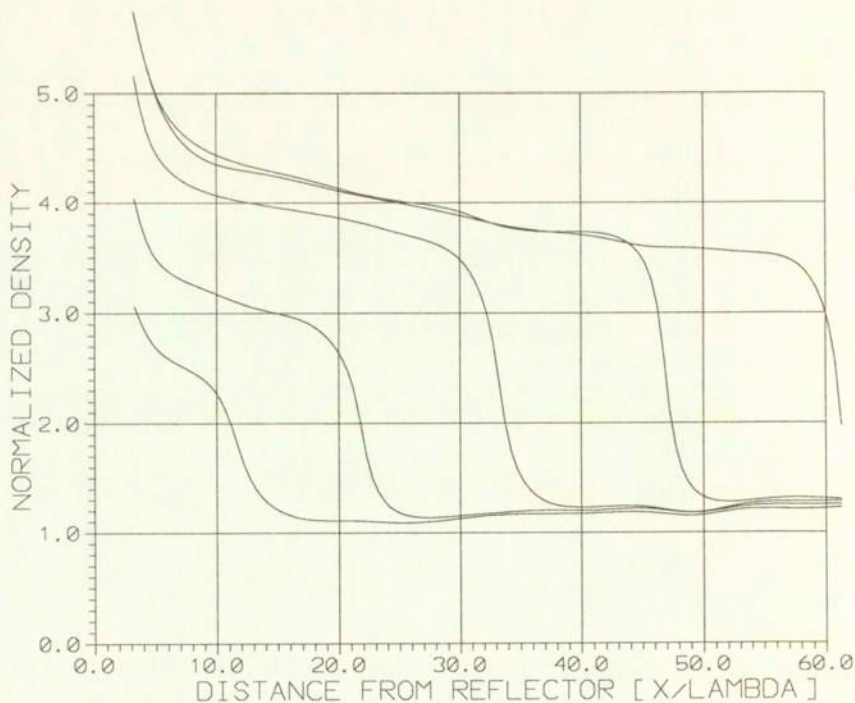FIG. 5. Reflected shock trajectories from experiment and DSMC calculations.

FIG. 6. Density distributions inside the reflected shock for shock positions specified in Fig. 4 (from experiment).

4.3. Monte–Carlo simulation

4.3.1. Parabolic reflector – results and comparison with experiment. The DSMC calculations of the reflected shock focusing were performed for the same flow conditions as the described experiment. The results are shown in the following figures. Figure 7 shows six instantaneous maps of the constant density isolines, five of them, a – e, correspond approximately to the situations shown in Fig. 4. Figure 5 (dashed line) presents the respective diagram of the reflected shock trajectory, while Fig. 8 the corresponding density distributions along the axis of the reflector (reflected shock wave structures at the axis). Figure 9 shows maps of isotherms, isobars and lines of constant values of horizontal and vertical (directed towards the plane of symmetry) velocity components for shock position corresponding to Fig. 7 d (maximum intensity of the shock at the axis).

The above figures allow us to understand the phenomena occurring in the neighbourhood of the shock focus. The gas, flowing in axial direction in the area behind the incident shock, turns towards the plane of symmetry when passing through the reflected one (compare Fig. 9 d, showing areas where gas velocity has vertical component directed towards the axis). Thus, behind the reflected shock two streams flow in opposite directions, meeting at the plane of symmetry. The highest pressure, temperature, density are produced there. In consequence, the reflected shock at the plane of symmetry is stronger than far from it. As the stronger shock moves faster with respect to the gas in front of it, the central part of the reflected shock becomes plane (Fig. 7 e) and then convex (Fig. 7 f). This takes place before the shock reaches the geometrical focus of the mirror and thus limits the focusing process.
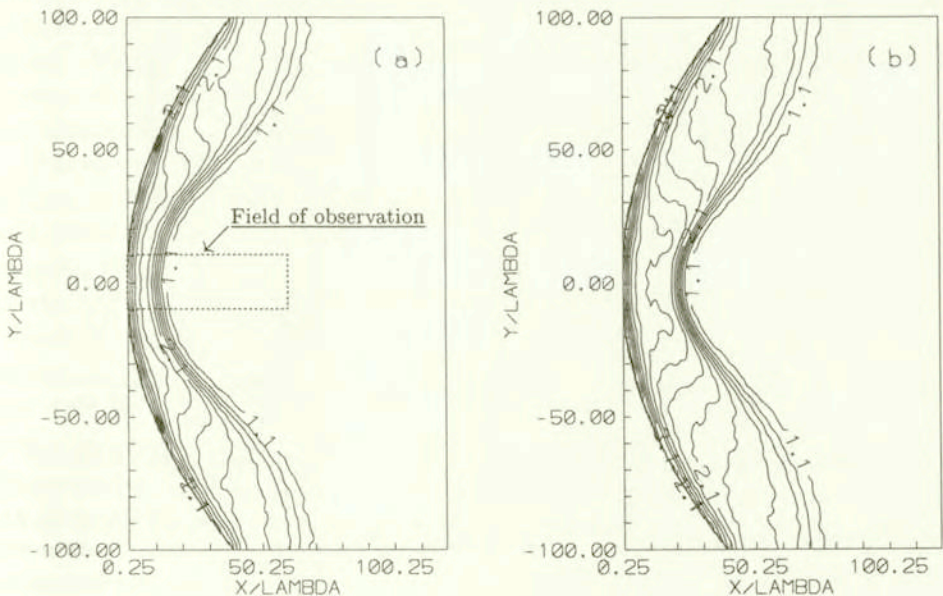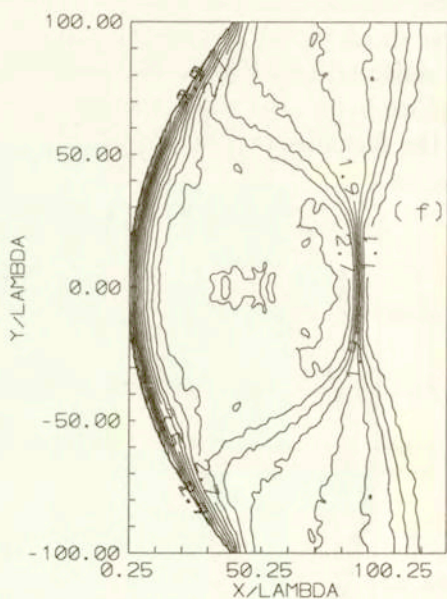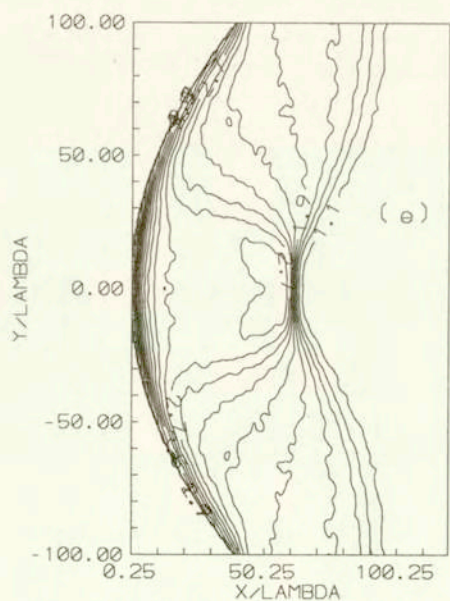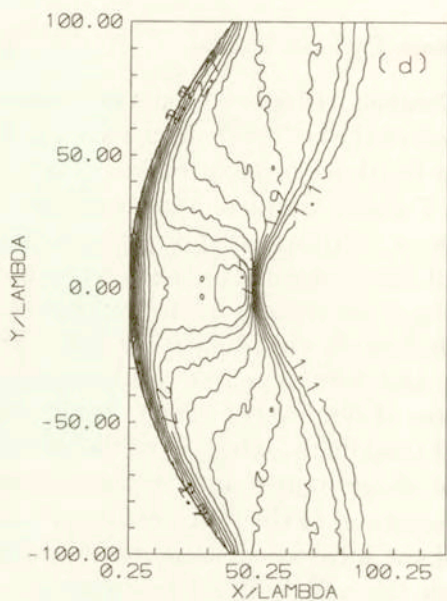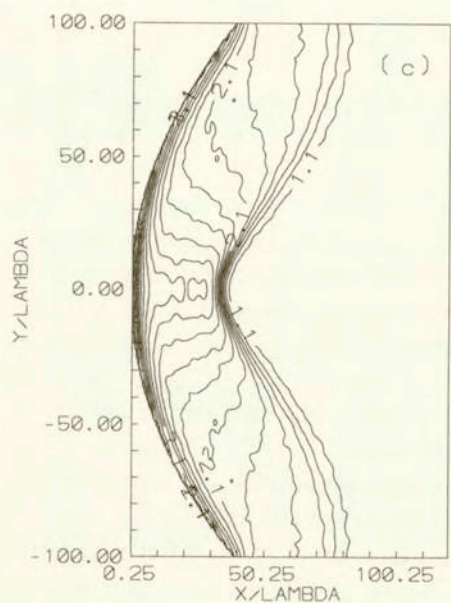

[FIG. 7 a, b]

FIG. 7. Constant normalized density contours ($\bar{\varrho}$) for six positions of the reflected shock (from DSMC calculations). Distances from the apex of the reflector to the centre of the reflected shock equal to: a) 11.1λ, b) 21.7λ, c) 33.4λ, d) 47.3λ, e) 61.0λ, f) 86.2λ.
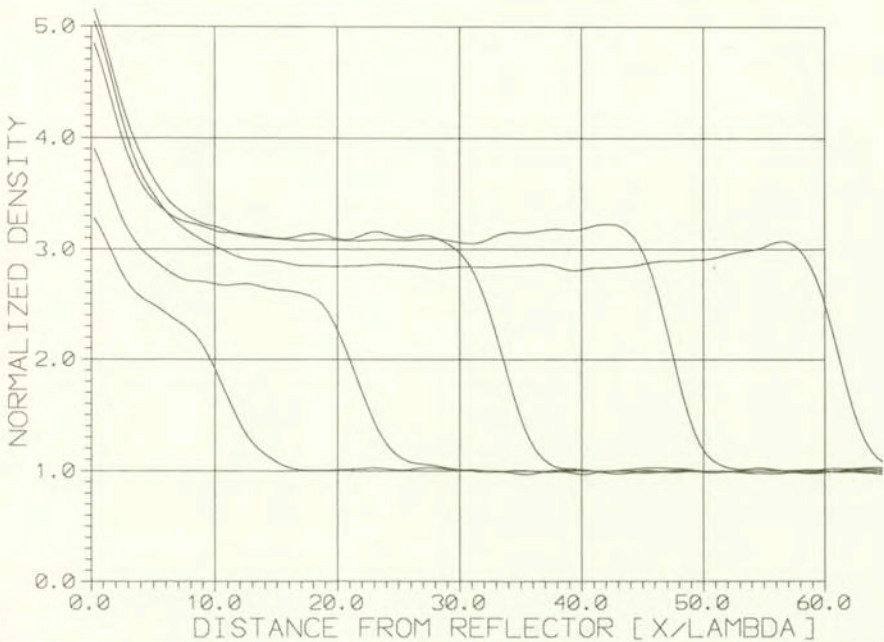
[274]

FIG. 8. Density distributions inside the reflected shock at the axis of the reflector,
for five shock positions specified in Fig. 7 a–e (from DSMC calculations).

Similar physical explanation is mentioned briefly by STURTEVANT and KUL-
KARNY [2] when they describe the differences between linear (geometrical) and
nonlinear approaches to the focusing of the shock wave. The behaviour of the
gasdynamic focus was briefly described by NISHIDA *et al.* [13], and the effects
of the changing shape (from the concave to the convex) could be seen on the
isobars shown by NISHIDA and KISHIGE [14] (their Figs. 3–5), but no physical
explanation was offered in these papers.

There is a good agreement between the Monte–Carlo simulation and experi-
mental results. The shapes of the constant density lines from experiment (Fig. 4)
and DSMC calculations (Fig. 7) show close resemblance, provided that one keeps
in mind that Fig. 4 presents only the narrow part of the flow field, corresponding
to the central part of Fig. 7 (as marked there by the dashed line). Actually, the
"shock focus" takes nearly the whole width of the experimental field of obser-
vation (Fig. 4). It may therefore be concluded, that dimension of the "focus" in
the direction perpendicular to the tube axis is equal to about 10–15 mean free
paths of the gas particles in front of the incident shock. Similar estimation can
be made on the basis of Fig. 7.

The shapes of the reflected shock trajectories from experiment and DSMC
simulation, as shown in Fig. 5, are also similar, although in the experiment the
reflected shock is definitely slower. The density distributions along the axis of
the reflector (Figs. 6 and 8) exhibit perhaps the most marked differences: the
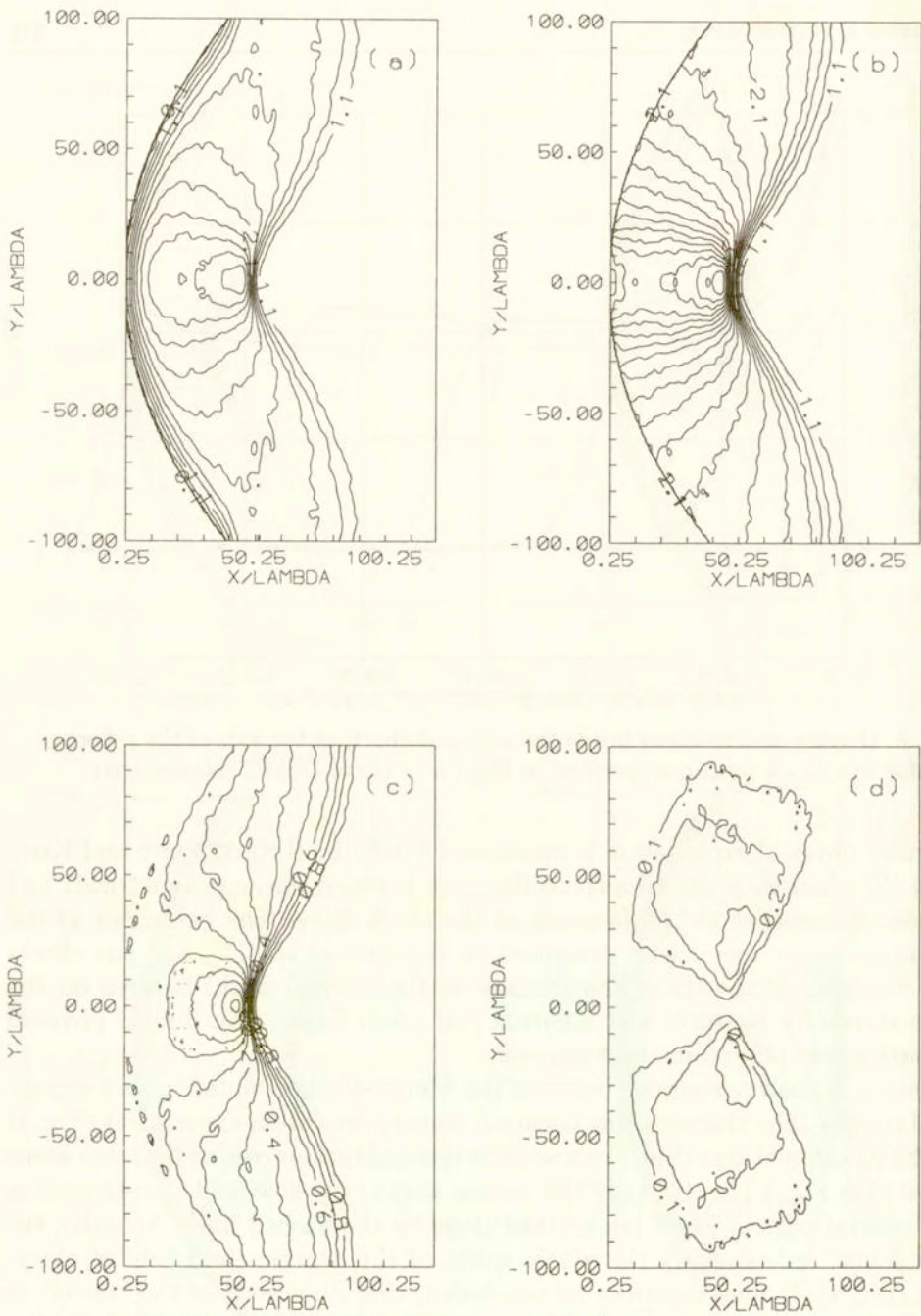
FIG. 9. Contours of constant normalized: a) temperature $(\overline{T})$, b) pressure $(\overline{p})$, c) horizontal $(\overline{u})$ and d) vertical $(\overline{v})$ velocity components for shock position specified in Fig. 7 d (from DSMC calculations).

[276]

density increase across the reflected shock is substantially higher in the experiment than in the simulation and, moreover, behind the reflected shock the gas density further increases, while in the simulation there is a definite minimum of density in this area.

The described differences result from flow nonuniformity in front of the reflected shock wave, clearly visible in Figs. 3 and 6 in the form of density variation in this area. This nonuniformity is due to the influence of boundary layer at the sidewalls of the shock tube. To verify this supposition, a relatively simple calculation was made of a plane shock wave, moving in a narrow channel with nonzero accommodation coefficient at the walls, reflecting from a plane endwall of the channel. The results indicate both the increase of gas density behind the incident shock, and the increase of density behind the reflected shock. Similar effect has also been obtained experimentally by PIVA [15].

One more point should be mentioned here: in the reported experiment the reflector did not span the whole distance between the walls of the shock tube (Fig. 1), as it did in the simulation (Fig. 2). To check what influence it could have upon the focusing process, additional calculations were performed for suitable geometry. The obtained results indicate, that noticeable differences are visible only in the vicinity of the edges of the reflector. The density distributions along the axis of the reflector for this geometry are nearly identical with those for the standard case, shown in Fig. 8. It should be pointed out here, that STURTEVANT and KULKARNY [2] obtained a similar result experimentally.

4.3.2. Other shapes of the reflector. Calculations described up to this point were done for parabolic reflectors. This shape, however, was obtained from geometrical acoustics (linear theory); it is not necessarily the best one for reflecting shock waves (nonlinear phenomena). It was therefore interesting to see the shock focusing with reflectors of other shapes. Apart from that, as no technologically produced shape is perfect, it was important from the practical point of view to know the effect of the possible inaccuracy of the shape of the reflector.

The calculations were performed for reflectors of the same depth as before, with shapes described by the equation:

$$x = c\,y^{\beta},$$

where x – coordinate along the shock tube axis, y – distance from the plane of symmetry. Exponent β was taken equal to 1.5 and 2.5, constant c was calculated to obtain the required depth of the reflector.

The results are quite similar to those for a parabolic reflector. To explain it we inspected carefully the considered shapes. We found, that for the same distances from the plane of symmetry (y-coordinate), the differences between the corresponding x-coordinates were smaller than the size of the "focus". Most probably then, in order to influence the phenomenon more substantially, the

disturbance of the shape of the reflector would have to be much larger than the dimension of the focus.

5. Comparison with high-density results

The results presented here, both experimental and numerical, agree qualitatively with those of other authors for high gas densities. The shapes of the waves from Monte–Carlo simulation (Fig. 7) are similar to those obtained for strong shocks experimentally by Sturtevant and Kulkarny ([2] – Fig. 4 of that paper), or numerically by Nishida and Kishige ([14] – Fig. 4 there). Similarly, our experimental results (Fig. 4) agree with corresponding parts of their pictures.

Exact quantitative comparison is, unfortunately, impossible because of different geometrical and flow conditions (depth of the reflector, shock Mach number, gas density). The most visible difference is, of course, that at low density all waves are of finite thickness, "more widely spread". Still, the waves visible at high-density pictures of the flow can also be recognized at low densities (unless they are too weak to be detected). Hence, it may be stated, that the present investigation in the rarefied flow regime confirms the results known from research at high gas density.

6. Conclusions

1. The presented experimental results supply the information about the process of formation, size and structure of the focus of the "strong" shock after its reflection from a concave wall.

2. The results of the DSMC simulation are in good agreement with experiment. They make it also possible to understand the mechanism of focusing a shock after reflection, with all its inherent limitations. In particular, the fact that the shock after reflection from a concave wall is never uniformly strong, puts the lower bound upon the size of the focus which, in turn, limits the maximum intensity of the focused shock.

3. The present results agree qualitatively with results of other authors, both experimental and numerical, obtained for high density gases.

Acknowledgments

References

1. R.W. PERRY and A. KANTROWITZ, *The production and stability of converging shock waves*, J. Appl. Phys., **22**, 878–886, 1951.

2. B. STURTEVANT and V.A. KULKARNY, *The focusing of weak shock waves*, J. Fluid Mech., **73**, 4, 651–671, 1976.

3. R. HOLL and H. GRONIG, *Focusing of weak blast waves*, pp. 563–570, Proc. 14th Int. Symp. on Shock Tubes and Waves, Sydney 1983.

4. H. GRONIG, *Shock wave focusing phenomena*, pp. 878–886, Proc. 15th Int. Symp. on Shock Waves and Shock Tubes, Berkeley, California 1985.

5. *Shock tube of the IFTR* [in Polish], Prace IPPT 47/1976, 1976.

6. H.N. BALLARD and D. VENABLE, *Shock front thickness measurements by an electron beam technique*, Phys. Fluids, **1**, 3, 225–229, 1958.

7. W. FISZDON, R. HERCZYŃSKI and Z. WALENTA, *The structure of a plane shock wave of a monatomic gas. Theory and experiment*, Proc. 9-th Int. RGD Symp., Goettingen 1974.

8. G.A. BIRD, *Molecular gas dynamics*, Clarendon Press, Oxford 1976.

9. V.E. YANITSKIY and O.M. BELOTSERKOVSKIY, *The statistical method of particles in cells for the solution of problems of the dynamics of a rarefied gas.* Part I, Zh. Vychisl. Mat. Mat. Fiz., **15**, 1195–1208; Part II, Zh. Vychisl. Mat. Mat. Fiz., **15**, 1553–1567, 1975.

10. J.C. MAXWELL, *The scientific papers of James Clerk Maxwell* W.D. NIVEN [Ed.], New York, Dover, **2**, 706, 1952.

11. H. HONMA, D.Q. XU and T. ABE, *DSMC approach to nonstationary Mach reflection of strong incoming shock waves using a smoothing technique*, Shock Waves, **3**, 67–72, 1993.

12. K. KANTIEM, A. KOZŁOWSKI and Z.A. WALENTA, *Reflection of a moving shock wave; boundary conditions for Monte–Carlo and continuum descriptions*, Arch. Mech., **47**, 1, 69–80, 1995.

13. M. NISHIDA, T. NAKAGAWA, T. SAITO and M. SOMMERFELD, *Interaction of weak shock waves reflected on concave walls*, pp. 211–217, Proc. 15th Int. Symp. on Shock Waves and Shock Tubes, Berkeley, California 1985.

14. M. NISHIDA and H. KISHIGE, *Numerical simulation of focusing process of reflected shock waves*, pp. 551–557, Proc. 16th Int. Symp. on Shock Tubes and Waves, Aachen, Germany 1987.

15. H. DE OLIVEIRA PIVA, *Electron beam measurements of density in shock waves reflecting from a cold wall*, Ph.D. Thesis, Cal. Inst. of Technology, May 17, 1968.

16. V.V. SERIKOV, *Private communication*.

POLISH ACADEMY OF SCIENCES
INSTITUTE OF FUNDAMENTAL TECHNOLOGICAL RESEARCH
e-mail: zwalenta@ippt.gov.pl